

# A New Approach to GraphMaps, a System Browsing Large Graphs as Interactive Maps

Debajyoti Mondal<sup>1</sup> and Lev Nachmanson<sup>2</sup>

<sup>1</sup>Cheriton School of Computer Science, University of Waterloo, Canada,  
dmondal@uwaterloo.ca

<sup>2</sup>Microsoft Research, Redmond, USA, levnach@microsoft.com

May 17, 2017

## Abstract

Visualization of large graphs has become increasingly important due to the growing size of data available around us. Traditional data visualization systems render the graph in full detail on a single screen. This approach sometimes requires to render many objects on the screen, which overwhelms the user. A GraphMaps system tries to overcome this problem by visualizing the graph using zoom levels, which is similar to a geographic map visualization. GraphMaps reveals the structural properties of the graph and enables users to interact with the graph in a natural way. The available implementation of GraphMaps system is based on an incremental mesh generation technique that does not control the number of zoom levels and the way the nodes appear on different levels.

In this paper we develop a technique to construct GraphMaps from any given mesh that is generated from a 2D point set, and for any given number of zoom levels. We demonstrate our approach introducing competition mesh, which is simple to construct, has low dilation and high angular resolution. Finally, we give an algorithm for assigning nodes to zoom levels that minimizes the number of nodes appearing while the user zooms in to a lower level. Keeping the number of such nodes low helps avoiding abrupt changes when zooming in and out between the levels.

## 1 Introduction

We first review the major features of GraphMaps, and give some definitions. The system confronts the challenge of visualizing large graphs by enabling the users to browse the graphs as interactive maps. Like Google or Bing Maps the GraphMaps system visualizes the high priority features on the top level, and as we zoom in, the low priority entities start to appear in the subsequent levels. To achieve this effect, for a given graph  $G$  and a positive integer  $k > 0$ , GraphMaps creates the graphs  $G_1, G_2, \dots, G_k$ , where  $G_i$ ,  $1 \leq i < k$ , is an induced subgraph of  $G_{i+1}$ , and  $G_k = G$ .

The graph  $G_i$ , where  $1 \leq i \leq k$ , corresponds to the  $i$ th zoom level. Assume that the nodes of  $G$  are ranked by their importance. The discussion on what a node importance is and how the ranking is obtained, is out of the scope of the paper, but by default GraphMaps uses Pagerank [6] to obtain such a ranking. Let  $V(G_i)$  be the nodes of  $G_i$ . We build graphs  $G_i$  in such a way that the nodes of  $G_i$  are equally or more important than the nodes of  $V(G_{i+1}) \setminus V(G_i)$ . At the top view, we render the graph  $G_1$ . As we zoom in and the zoom reaches  $2^{i-1}$ , the rendering switches from  $G_{i-1}$  to  $G_i$ , exposing less important nodes and their incident edges. To create spatial stability GraphMaps keeps the node positions fixed, and the rendering of edges changes incrementally between  $G_i$  and  $G_{i+1}$  as described in Section 3.

By browsing a graph with GraphMaps, the user obtains a quick overview of the important elements. Navigation through different zoom levels reveals the structure of the graph. In addition, users can interact with the system. For example, when the user clicks on a node  $u$ , the

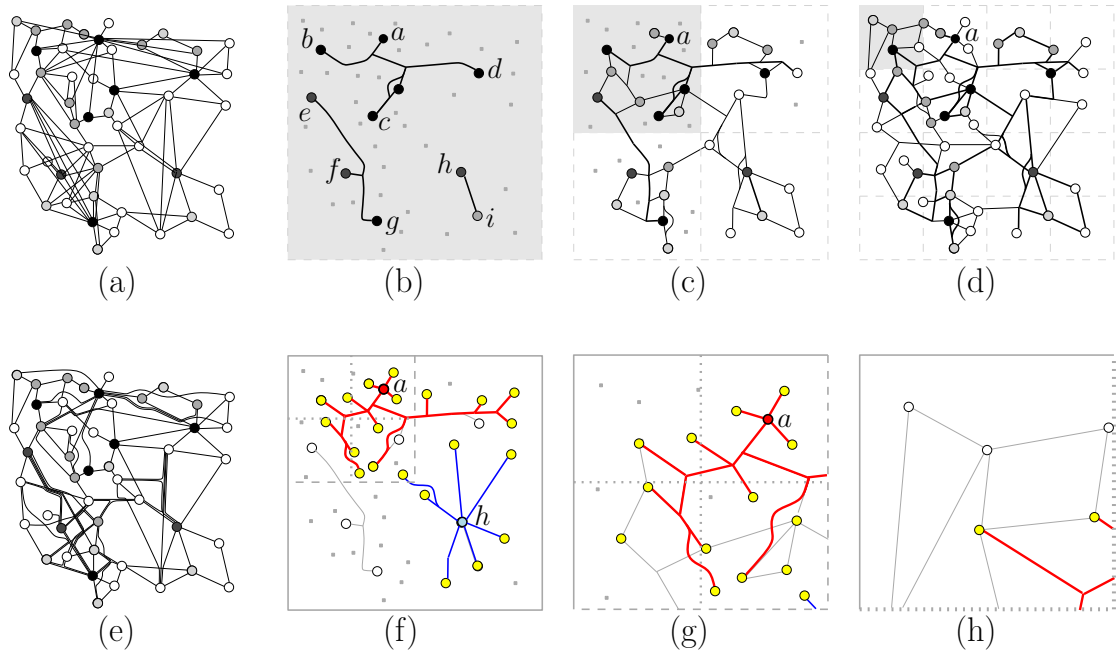


Figure 1: (a) A traditional node-link diagram of a graph  $G$ . (b–d) A GraphMaps visualization of  $G$ . (e) An example of edge bundling. (f–h) Illustration for node selections and zoom in.

visualization highlights and renders all neighbors of  $u$  (even those that do not belong to the current  $G_i$ ) and the edges that connect  $u$  to its neighbors. By using this interaction the user can explore a path by selecting a set of successive nodes on the path, and can answer adjacency questions by selecting the corresponding pair of nodes.

We draw the nodes as points, and edges as polygonal chains. Each maximal straight line segment in the drawing is called a *rail*. The edges may share rails, but no edge passes through a node. Every point where a pair of rails meet is either a node or a point which we call a *junction*. Figure 1(a) depicts a traditional node-link diagram of a graph  $G$ . Figures 1(b–c) illustrate a GraphMaps visualization of  $G$  on three zoom levels. The gray region at each level corresponds to a viewport in that level. The higher ranked nodes of  $G$  have the darker color. The tiny gray dots represent the locations of the nodes that are not visible in the current layer. Figures 1(f–h) illustrate the node selection technique and the zoom feature. The rails rendered by thick lines correspond to the shortest path tree from the selected nodes  $a$  and  $h$  to their neighbors.

In our scheme, where we change the rendering depending on the zoom level, the quality of the visualization depends both on the quality of the drawing on each level, and the differences between the drawings of successive zoom levels. We think that a good drawing of a graph on a single zoom level satisfies the following properties:

- The angular resolution is large
- The *degree* at a node or at a junction is small.
- The amount of *ink*, that is the sum of the lengths of all distinct rails used in the drawing, is small.
- The *edge stretch factor* or *dilation*, that is the ratio of the length of an edge route to the Euclidean distance between its end nodes, is small.

These properties help to follow the edge routes, reduce the visual load, and thus improve the readability of a drawing. However, since some of the principles contradict each other, optimizing all of them simultaneously is a difficult task. In Appendix A, we demonstrate these challenges through a toy example of GraphMaps.

Our algorithm, in addition to creating a good drawing of each  $G_i$ , attempts to construct these drawings in a way that a switch from  $G_i$  to  $G_{i+1}$  does not cause a large change on the screen. We try to keep the amount of new appearing details relatively small and also try to keep the edge geometry stable. We created a video <sup>1</sup> to demonstrate the new version of GraphMaps. The GraphMaps system used to develop this video does not integrate the node assignment technique described in Section 4.

## Related Work

A large number of graph visualization tools and techniques [1, 2, 3, 4] have been developed over the past few decades due to a growing interest in exploring network data. Many of these tools provide a rich interaction set, and are very useful to visualize moderate size graphs. On the contrary, only a few tools support large graphs, e.g., graphs having several thousands of nodes and edges. One obvious reason for that is that the naive approach to rendering does not work any more. After rendering all the entities at once, it becomes very difficult to interact with the visualization.

A good visualization requires the nodes to be placed in some meaningful places, e.g., sometimes nodes with similar properties are placed close to each other, whereas the nodes that are dissimilar are placed far away. Force directed approaches, multi-dimensional scaling and stochastic neighbor embedding are some common techniques to generate the node positions [18, 19, 25]. Techniques that try to make the visualization readable by drawing the edges carefully include various types of edge bundling [13, 20, 24] and edge routing techniques [8, 17, 10]. Informally, the edge bundling technique groups the edges that are travelling towards a common direction, and routes these edges through some narrow tunnel. Figure 1(e) shows how edge bundling could be used to enhance the clarity of the visualization of Figure 1(a).

GraphMaps was proposed by Nachmanson et al. [21], where they use multidimensional scaling to create the node positions. They consider at each level  $i$ , an uniform  $2^i \times 2^i$  grid, where each grid cell is called a *tile*. The tiles are filled with nodes, the most important nodes first. While filling the levels with nodes, they maintain a node and a rail quota that bound the number of nodes and rails intersecting a tile. Whenever an insertion of a new node creates a tile intersecting more than one fourth of the node quota nodes or more than one quarter of rail quota rails, a new zoom level is created to insert the rest of the entities. The visualization of GraphMaps works in such a way that each viewport is covered by four tiles of the current level. This ensures that not more than the node quota nodes and the rail quota rails are rendered per viewport.

Some systems render large graphs on multiple layers by using the notion of temporal graphs, for example, evolving software system [7, 20]. A generalization of stochastic neighbor embedding renders nodes on multiple maps [26]. Gansner et al. [12] proposed a visualization that emphasizes node clusters as geographic regions. However, all these approaches are different from GraphMaps with respect to the goals a GraphMaps system tries to achieve.

## Contribution

The previous work on GraphMaps [21] focused mainly on the quality of the layout at individual zoom level. The construction followed a top-down approach, where the successive levels were obtained by inserting nodes incrementally in a greedy manner.

We propose an algorithm to construct a GraphMaps visualization starting from a complete drawing of the graph  $G(= G_k)$  at the bottom level. Specifically, given an arbitrary mesh and the edge routes of  $G_k$  on this mesh, our method builds the edge routes for  $G_{k-1}, \dots, G_2, G_1$ , in this order.

We introduce a particular type of mesh, called competition mesh, which is of independent interest due to its low edge stretch factor ( $2 + \sqrt{2}$ ), and high angular resolution  $45^\circ$ . We then construct GraphMaps visualizations by applying our algorithm to this mesh.

We develop a node assignment algorithm that minimizes the change in the drawing when switching from  $G_i$  to  $G_{i+1}$  during the zoom in operation, where  $1 \leq i < k$ .

<sup>1</sup><https://www.youtube.com/watch?v=vWaomeSDyTE>

## 2 Technical Background

We now introduce the mesh that we use for edge routing and analyze its properties. Let  $P$  be a set of  $n$  distinct points that correspond to the node positions, and let  $R(P)$  be the smallest axis aligned rectangle that encloses all the points of  $P$ . A *competition mesh* of  $P$  is a geometric graph constructed by shooting from each point, four axis-aligned rays at the same constant speed (towards the top, bottom, left and right), where each ray stops as soon as it hits any other ray or  $R(P)$ . We break the ties arbitrarily, i.e., if two non-parallel rays hit each other simultaneously, then arbitrarily one of these rays stops and the other ray continues. If two rays are collinear and hit each other from the opposite sides, then both rays stop. We denote this graph by  $M(P)$ . The vertices of  $M(P)$  are the points of  $P$  (*nodes*), and the points where a pair of the rays meet (*junctions*). Two vertices in  $M(P)$  are adjacent if and only if the straight line segment connecting them belongs to  $M(P)$ . A competition mesh can also be viewed as a variation of a motorcycle graph [11]. Figure 2 illustrates a competition mesh of 8 points. Throughout this paper we use the term ‘vertices’ to denote all the nodes and junctions of the mesh.

For any point  $u$ , let  $u_x$  and  $u_y$  be the  $x$  and  $y$ -coordinates of  $u$ , respectively, and let  $l_v(u)$  and  $l_h(u)$  be the vertical and horizontal straight lines through  $u$ , respectively. For any two points  $p, q$  in  $\mathbb{R}^2$ , let  $dist_E(p, q)$  (respectively,  $dist_M(p, q)$ ) be the Euclidean distance (respectively, Manhattan distance) between  $p$  and  $q$ . For each point  $u$  of the plane we define four *quadrants* formed by the horizontal and vertical lines passing through  $u$ . A path  $v_1, \dots, v_k$  is *monotone* in direction of vector  $\mathbf{a}$  if for each  $1 \leq i < k$  the dot product  $\mathbf{a} \cdot (v_{i+1} - v_i)$  is not negative. The following lemmas prove some properties of  $M(P)$ .

**Lemma 1** *Let  $u$  be a node in  $M(P)$ . Then in each quadrant of  $u$  there is a path in  $M(P)$  that starts at  $u$ , ends at some point on  $R(P)$ , and is monotone in both horizontal and vertical directions.*

**Proof:** Without loss of generality it suffices to prove the lemma for the first quadrant of  $u$ , which consists of the set of points  $v$  such that  $v_x \geq u_x$  and  $v_y \geq u_y$ . Suppose for a contradiction that there is no such path in this quadrant. Consider a maximal  $xy$ -monotone path  $\Pi$  that starts at  $u$  and ends at some node or junction  $w$  of  $M(P)$ . If  $w$  is a node, then we extend  $\Pi$  using the right or top ray of  $w$ , which is a contradiction. Therefore,  $w$  must be a junction in  $M(P)$ . Without loss of generality assume that the straight line segment  $\ell$  incident to  $w$  is horizontal. Since  $\Pi$  is a maximal  $xy$ -monotone path, the ray  $r_\ell$  corresponding to  $\ell$  must be stopped by some vertical ray  $r'$  generated by some vertex  $w'$ . Observe that  $w_y > w'_y$ , otherwise we can extend  $\Pi$  towards  $w'$ . Since  $r_\ell$  is stopped, the ray  $r'$  must continue unless there are some other downward ray  $r''$  that hits  $r'$  at  $w$ . In both cases we can extend  $\Pi$ , either by following  $r'$  (if it continues), or following the source of  $r''$  (if  $r'$  is stopped by  $r''$ ), which contradicts to the assumption that  $\Pi$  is maximal.  $\square$

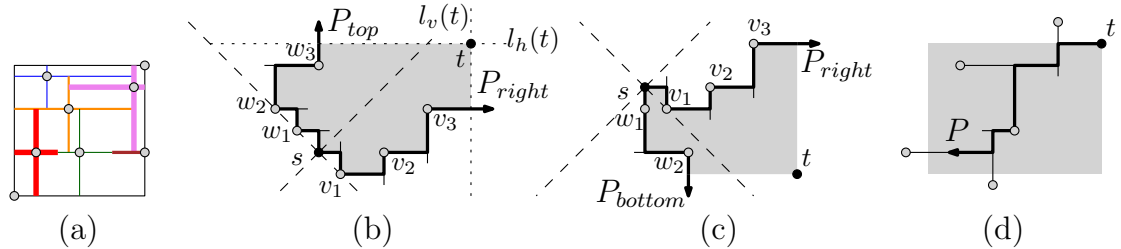


Figure 2: (a) A point set and its corresponding competition mesh. (b–c) Bounding the bottom-left quadrant of  $t$ . (d) A monotone path inside the bottom-left quadrant of  $t$ .

**Lemma 2** *For any set  $P$  with  $n$  points  $M(P)$  has  $O(n)$  vertices and edges. Furthermore, the graph distance between any two nodes of  $M(P)$  is at most  $(2 + \sqrt{2})$  times the Euclidean distance.*

**Proof:** By construction of  $M(P)$ , whenever a junction is created one ray stops. Since  $|P| = n$  there are at most  $4n$  rails, and therefore we cannot have more than  $4n$  junctions, that proves that the number of vertices in  $M(P)$  is  $O(n)$ . Since  $M$  is a planar graph, the number of edges is also  $O(n)$ .

We now show that the ratio of the graph distance and the Euclidean distance between any two nodes of  $M(P)$  is at most  $(2 + \sqrt{2})$ . Let  $C_{left}, C_{right}, C_{top}$ , and  $C_{bottom}$  be the four cones with the apex at  $(0, 0)$  determined by the lines  $y = \pm x$ . Let  $s$  and  $t$  be two nodes in  $M(P)$ . Without loss of generality assume that  $s$  located at  $(0, 0)$  and  $t$  lies on  $C_{right}$ . Consider now an  $x$ -monotone orthogonal path  $P_{right} = (v_0, v_1, v_2, \dots, v_t)$  in the mesh such that  $v_0$  coincides with  $s$ , for each  $0 < i \leq t$ ,  $v_i$  is a node in  $M(P)$  that stops the rightward ray of  $v_{i-1}$ , and  $v_t$  lies on or to the right of  $l_v(t)$ , as shown in Figure 2(b). Suppose that  $t$  is either above or below  $P_{right}$ . If  $t$  is above  $P_{right}$ , then we consider a  $y$ -monotone path  $P_{top} = (w_0, w_1, w_2, \dots, w_t)$  such that  $w_0$  coincides with  $s$ , for each  $0 < i \leq t$ ,  $w_i$  is a node in  $M(P)$  that stops the upward ray of  $v_{i-1}$ , and  $v_t$  lies on or above  $l_h(t)$ . If  $t$  is below  $P_{right}$ , then we can define a path  $P_{bottom}$  symmetrically, as shown in Figure 2(c).

Without loss of generality assume that  $t$  is above  $P_{right}$ . Observe that the paths  $P_{top}$  and  $P_{right}$  remain inside the cones  $C_{top}$  and  $C_{right}$ , respectively, and bound the bottom-left quadrant of  $t$ , as shown in the shaded region in Figure 2(b). By Lemma 1,  $t$  has a  $(-x)(-y)$ -monotone path  $P$  that starts at  $t$  and reaches the boundary of  $R(P)$ , e.g., see Figure 2(d). This path  $P$  must intersect either  $P_{top}$  or  $P_{right}$ . Hence we can find a path  $P'$  from  $s$  to  $t$ , where  $P'$  starts at  $s$ , travels along either  $P_{top}$  or  $P_{right}$  depending on which one  $P$  intersects, and then follows  $P$  from the intersection point. We now show that length of  $P'$  is at most  $(2 + \sqrt{2}) \cdot dist_E(s, t)$ . Since any ray is not shorter than a ray it stops, the sum of the lengths of the vertical segments of  $P_{right}$  is at most the sum of the lengths of the horizontal segments. Therefore, the part of  $P_{right}$  inside the bottom-left quadrant of  $t$  is at most  $2t_x$ . Similarly, the part of  $P_{top}$  inside the bottom-left quadrant of  $t$  is at most  $2t_y$ . Path  $P$  is not longer than  $t_x + t_y$  (see Figure 2(d)). Therefore, the length of  $P'$  is at most

$$\begin{aligned} & t_x + t_y + 2 \cdot \max\{t_x, t_y\} \\ & \leq \sqrt{2} \cdot dist_E(s, t) + 2 \cdot \max\{t_x, t_y\} \\ & \leq (2 + \sqrt{2}) \cdot dist_E(s, t). \end{aligned}$$

In the case when  $t$  belongs to  $P_{right}$ , the length of path  $P$  is zero and the proof easily follows.  $\square$

The following lemma states that a competition mesh can be constructed in  $O(n \log n)$  time, whose proof is included in the Appendix B.

**Lemma 3** *A competition mesh  $M$  of a set  $P$  of  $n$  points can be constructed in  $O(n \log n)$  time.*

In the subsequent sections, we describe how the competition mesh is used in GraphMaps.

### 3 GraphMaps System Based on Competition Mesh

Our technique for calculating the graphs  $G_1, \dots, G_k$  is described in Section 4. For now, let us assume that the sequence of graphs is ready. We now show how to route edges on graphs  $G_i$ .

#### 3.1 Edge Routing and Local Modifications

The computation of edges starts from the bottom. Namely we build a competition mesh  $M$  for graph  $G(= G_k)$ . We route each edge  $(u, v) \in G$  as a shortest path  $P_{uv}$  in  $M$ . Path  $P_{uv}$  should not pass through another node of  $G$ , otherwise the visualization would show some edges that do not exist in  $G$ . To achieve this property, we surround each node of  $G$  by a polygon that creates a detour for  $P_{u,v}$ , and while routing, forbid  $P_{u,v}$  to enter a node distinct from  $u$  and  $v$ . Hence, the routing in fact runs on the modified  $M$ . Figures 3(a-c) illustrate an example where  $P_{uv}$  avoids the nodes  $a$  and  $b$ . After routing all edges of  $G$ , we remove from  $M$  every edge that is not used by a route  $P_{u,v}$  for any edge  $(u, v)$  of  $G$ .

Let us denote by  $M'$  the mesh we obtain after applying these modifications to  $M$ . Next we modify  $M'$  to make the routes more visually appealing. We perform local modifications and try to minimize the total ink of the routes, which is the sum of lengths of edges of  $M'$  used in the routes [14], and remove thin faces. During the modifications we keep the angular resolution greater or equal than some  $\alpha > 0$ , and the minimum distance between non-incident vertices and edges of  $M'$  greater or equal than some  $\beta > 0$ . The local modifications are described below.

**Face refinement:** For each face  $f$  of  $M'$  that does not contain a node of  $G$  in its boundary, we compute the width of  $f$ , which is the smallest Euclidean distance between any two non-adjacent rails of  $f$ . If the width of  $f$  is smaller than some given threshold, then remove the longest edge of  $f$  from  $M'$ . Figures 3(d-e) depict such a removal, where the thin face is shown in gray. The edge routes using the removed edge are rerouted through the remaining boundary of  $f'$ .

**Median:** Move each junction  $\kappa$  of  $M'$  toward the geometric median of its neighbors, i.e., the point that minimizes the sum of distance to the neighbors, as long as the restriction mentioned above holds. Iterate the move for a certain number of times, or until the change becomes very small. Figures 3(e-f) illustrate the outcome of this step.

**Shortcut:** Remove every degree two junction and replace the two edges adjacent to it by the edge shortcutting the removed junction, as long as the restriction mentioned above holds.

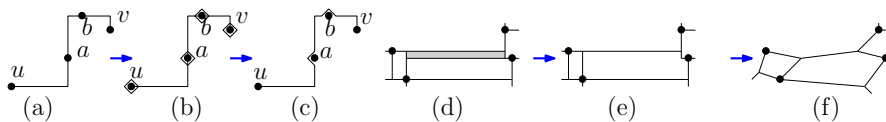


Figure 3: (a-c) Computing shortcut paths with detour. (d-e) Removal of thin faces. (e-f) Moving junctions towards geometric median.

In all the above modifications, the routes are updated accordingly. Modifications “Median” and “Shortcut” diminish the ink. The final  $M'$  gives the geometry of the bottom-level drawing of  $G$  in our version of GraphMaps.

### 3.2 Path Simplification and Transition between Successive Levels

Given a mesh  $M_i$  representing the geometry for the drawing of  $G_i$ , where  $1 < i \leq k$ , we construct  $M_{i-1}$  from  $M_i$  by removing from the latter the nodes  $V(G_i) \setminus V(G_{i-1})$ , and by removing the edges that are not used by any route  $P_{u,v}$ , where  $(u, v)$  is an edge of  $G_{i-1}$ . Some routes  $P_{u,v}$  can be straightened in  $M_{i-1}$ . We use the simplification algorithm [9] to morph the paths of  $M_i$  to paths of  $M_{i-1}$ . Figures 4(a-b) illustrate the simplification.

This change in the edge routes geometry diminishes the consistency between the drawings of successive levels. To smoothen the differences while transiting from zoom level  $i$  to  $i + 1$  we linearly interpolate between the paths of  $M_i$  and  $M_{i+1}$ , as demonstrated in Figures 4(b-d).

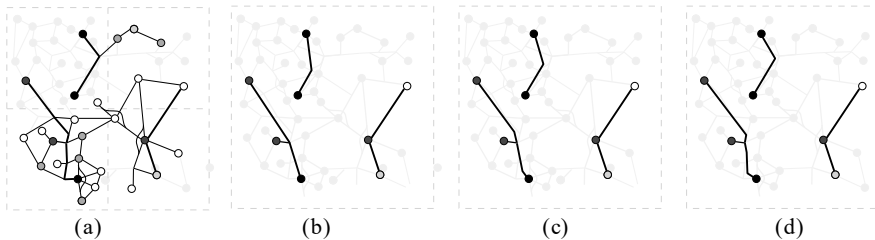


Figure 4: (a) Zoom level 2. (b-d) Transition from level 2 to 1.

The idea of path simplification and transition via linear interpolation enables us to construct GraphMaps in a bottom-up approach. In fact, the above strategy can be applied to transform any mesh generated from a set of 2D points to a GraphMaps visualization.

## 4 Computing Zoom Levels for Nodes

Let us consider in more details how the view changes when we zoom by examining Figure 5(a)–(d). On the top-left tile of Figure 5(a), the user’s viewport covers the whole graph, so  $G_1$  is exposed. In Figure 5(d), the user’s viewport contains only the top-left tile of Figure 5(a), and the visualization switches to graph  $G_2$ . Seven new nodes, which were not fully visible in zoom level 1, become fully visible for the current viewport, as represented in light gray. If all of a sudden, a large number of new nodes become fully visible, then it may disrupt user’s mental map. Here we propose an algorithm to keep this change small.

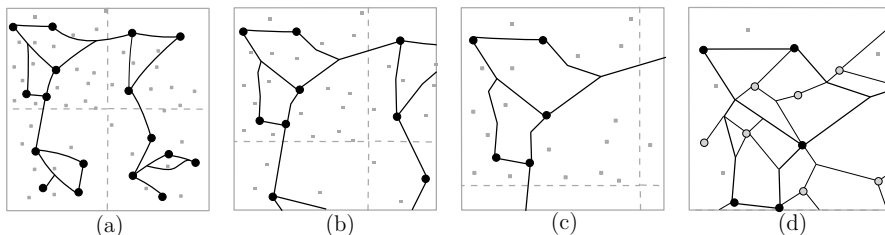


Figure 5: (a) Zoom level 1. (b–c) Transition from level 1 to 2. (d) Zoom level 2.

We build the tiles as in [21]. In the first level we have only one tile coinciding with the graph bounding box. On the  $i$ th level, where  $i > 1$ , the tiles are obtained by splitting each tile in the  $(i - 1)$ th level into a uniform  $2 \times 2$  grid cell. This arrangement of tiles can be considered as a rooted tree  $T$ , where the tiles correspond to the nodes of the tree. Specifically, the topmost tile is the root of  $T$ , and a node  $u$  is a child of another node  $v$  if the corresponding tiles  $t_u$  and  $t_v$  lie in two different but adjacent levels, and  $t_u \subset t_v$ . We refer to  $T$  as a *tile tree*.

For every node  $v$  in  $T$ , denote by  $S(v)$  the number of fully visible nodes in the tile  $t_v$ . For an edge  $e = (v, w)$  in  $T$ , where  $v$  is a parent of  $w$ , we denote by  $\delta_e$  the number of new nodes that become visible while navigating from  $t_v$  to  $t_w$ , i.e.,  $\delta_e = |S(w) \setminus S(v)|$ . We can control the rate the nodes appear and disappear from the viewport by minimizing  $\sum_{e \in E(T)} \delta_e^2$ , where  $E(T)$  is the set of edges in  $T$ . For simplicity we show how to solve the problem in one dimension, where all the points are lying on a horizontal line. It is straightforward to extend the technique in  $\mathbb{R}^2$ .

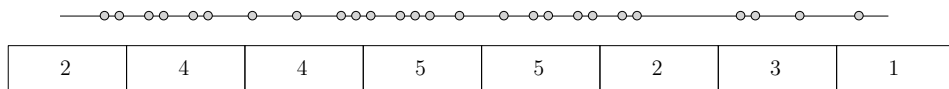
**Problem.** BALANCED VISUALIZATION

**Input.** A set  $P$  of  $n$  points on a horizontal line, where every point  $q \in P$  is assigned a rank  $r(q)$ . A tile tree  $T$  of height  $\rho$ ; and a node quota  $Q$ , i.e., the number of points allowed to appear in each tile.

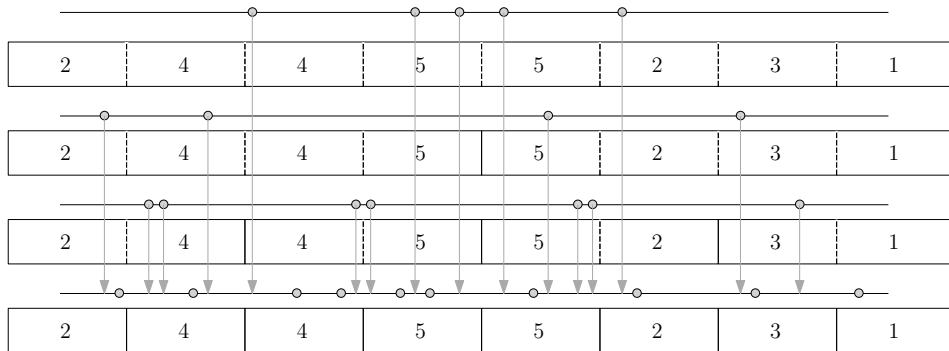
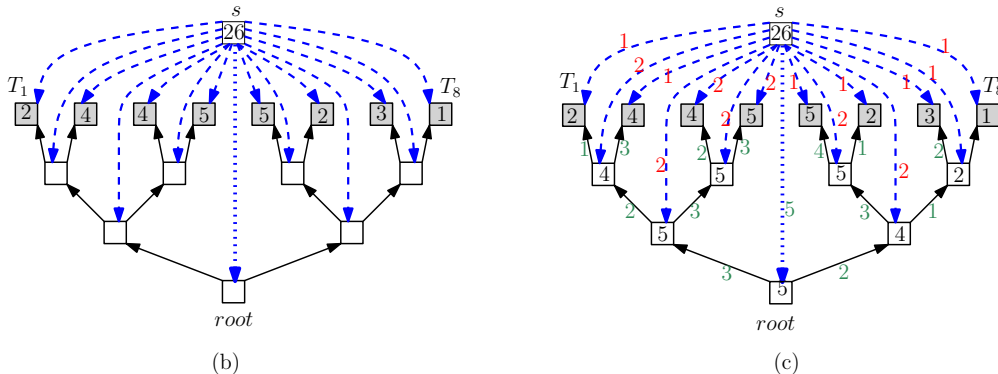
**Output.** Compute a mapping  $g : P \rightarrow \{1, 2, \dots, \rho\}$  (if exists) that

- satisfies the node quota,
- minimizes the objective function  $F = \sum_{e \in E(T)} \delta_e^2$ , and
- for every pair of points  $q, q' \in P$  with  $r(q) \geq r(q')$ , satisfies the inequality  $g(q) \leq g(q')$ , which we refer to as the *rank condition*.

If the rank of all the points are distinct, then the solution to BALANCED VISUALIZATION is unique, and can be computed in a greedy approach. But the problem becomes non-trivial when many points may have the same rank. In this scenario, we prove that the BALANCED VISUALIZATION problem can be solved in  $O(\tau^2 \log^2 \tau) + O(n \log n)$  time, where  $\tau$  is the number of nodes in  $T$ . This is quite fast since the maximum zoom level is a small number, i.e., at most



(a)



(d)

Figure 6: (a) A set of points on a line and the associated tiles are shown using rectangular regions. (b) A corresponding network  $G$ . (c) A solution to the minimum cost maximum flow problem. (d) A solution to the BALANCED VISUALIZATION problem that corresponds to the network flow.

10, in practice. We reduce the problem to the problem of computing a minimum cost maximum flow problem, where the edge costs can be convex [22, 23], e.g., quadratic function of the flow passing through the edge. Figure 6(a) depicts a set of points on a line, where the associated tiles are shown using rectangular regions. The numbers in each rectangle is the number of points in the corresponding tile. Figure 6(b) shows a corresponding network  $G$ , where the source is denoted by  $s$ , and the sinks are denoted by  $T_1, T_2, \dots, T_8$ .

The excess at the source and the deficit at the sinks are written in their associated squares. We allow each internal node  $w$  (unfilled square) of the tile tree to pass at most  $Q$  units of flow through it. This can be modeled by replacing  $w$  by an edge  $(u, v)$  of capacity  $Q$ , where all the edges incoming to  $w$  are incident to  $u$  and the outgoing edges are incident to  $v$ . This transformation is not shown in the figure. Set the capacity of all other edges to  $\infty$ .

The production of the source is  $n$  units, and the units of flow that each sink can consume is equal to the number of points lying in the corresponding tile. The cost of sending flows along the tree edges (solid black) is zero. The cost of sending flows along the dotted edge connecting the source and the tree root is also zero. The cost of sending  $x$  units of flow along the dashed edges is  $x^2$ ; sending  $x$  units of flow through a dashed edge corresponds to  $x$  new nodes that are becoming visible when we zoom in at the tile of the edge target. Figure 6(c) illustrates a solution to the minimum cost maximum flow problem, where the flows are interpreted as follows:

- (A) The number in a square denotes the number of points that would be visible in the associated tile.
- (B) The edges  $(s, w)$ , where  $w$  is not the root, are labeled by numbers. Each such number corresponds to the new nodes that will appear while zooming in from the tile associated to  $parent(w)$  to the tile associated to  $w$ . Thus the cost of this network flow is the sum of the squares of these numbers, i.e., 35.
- (C) Each edge of  $(u, v)$  of  $T$  is labeled by the number of nodes that are fully visible both  $u$  and in  $v$ .
- (D) Any one unit source-to-sink flow corresponds to a point of  $P$ , where the flow path  $source, u_1, u_2, \dots, u_k (= sink)$  denotes that the point appeared in all the tiles associated to  $u_1, \dots, u_k$ .

We now have the following lemma.

**Lemma 4** *A minimum cost maximum flow in  $G$  minimizes the objective function  $F$  of the BALANCED VISUALIZATION problem.*

**Proof:** If the amount of flow consumed at sink is smaller than  $n$ , then we can find a cut in  $G$  with total capacity less than  $n$ . Thus even if we saturate the corresponding tiles with points from  $P$ , we will not be able to visualize all the points without violating the node quota. Therefore, we can visualize all the points if and only if the flow is maximum and the total consumption is  $n$ . Therefore, the only concern is whether the solution with cost  $\lambda$  obtained from flow-network model minimizes the sum of the squared node differences between every parent and child tiles. Suppose for a contradiction that there exists another solution of BALANCED VISUALIZATION with cost  $\lambda' < \lambda$ . In this scenario we can label the edges of the network according to the interpretation used in (A)–(D) to obtain a maximum flow in  $G$  with cost  $\lambda'$ . Therefore, the minimum cost computed via the flow-network model cannot be  $\lambda$ , a contradiction.  $\square$

Given a solution to the network flow, we can construct a corresponding solution to the BALANCED VISUALIZATION problem as described below.

- For each point  $w$ , set  $g(w) = \infty$ .
- For each zoom level  $z$  from  $\rho$  to 1, process the tiles of zoom level  $z$  as follows. Let  $W$  be a tile in zoom level  $z$ . Find the amount of flow  $x$  incoming to  $W$  from  $s$  in  $G$ . Note that this amount  $x$  corresponds to the difference in the number of points between  $W$  and  $parent(W)$ . Therefore, we find a set  $L$  of  $x$  lowest priority points in  $W$  with zoom level equal to  $\infty$ , then for each  $w \in L$ , we set  $g(w) = z$ . Figure 6(d) illustrates a solution to the BALANCED VISUALIZATION problem that corresponds to the network flow of Figure 6(c).

If the resulting mapping does not satisfy the rank condition, then the instance of BALANCED VISUALIZATION does not have any affirmative solution. The best known running time for solving a convex cost network flow problem on a network of size  $O(\tau)$  is  $O(\tau^2 \log^2 \tau)$  [22, 23]. Besides, it is straightforward to compute the corresponding node assignments in  $O(n \log n)$  time augmenting the merge sort technique with basic data structures. Hence we obtain the following theorem.

**Theorem 1** *Given a set of  $n$  points in  $\mathbb{R}$ , a tile tree of  $\tau$  nodes, and a quota  $Q$ , one can find a balanced visualization (if exists) in  $O(\tau^2 \log^2 \tau) + O(n \log n)$  time.*

While implementing GraphMaps, we need to choose a node quota  $Q$  depending on the given total number of zoom levels  $\rho$ . Using a binary search on the number of nodes, in  $O(\log n)$  iterations, one can find a minimal node quota that allow visualizing all the points of  $P$  satisfying the rank condition.

## 5 Conclusion

We described our algorithm to construct GraphMaps Visualizations using competition mesh. Recall that the edge stretch factor of the competition mesh we created is at most  $(2 + \sqrt{2})$ . A natural open question is to establish tight bound on the edge stretch factor of the competition mesh. We refer the reader to [5] for more details on geometric mesh and spanners. We leave it as a future work to examine how the quality of a GraphMaps system may vary depending on the choice of geometric mesh.

For simplicity, we used polygonal chains to represent the edges, different colors for multiple node selections, and color transparency to avoid ambiguity. It would be interesting to find ways of improving the visual appeal of a GraphMaps visualization, e.g., using splines for edges, enabling tooltip texts for showing quick information and so on.

## References

- [1] Centrifuge systems. <http://centrifugesystems.com>, Accessed on June, 2016.
- [2] Cytoscape. <http://www.cytoscape.org>, Accessed on June, 2016.
- [3] Gephi. <http://gephi.github.io>, Accessed on June, 2016.
- [4] Graphviz. <http://graphviz.org>, Accessed on June, 2016.
- [5] Prosenjit Bose and Michiel H. M. Smid. On plane geometric spanners: A survey and open problems. *Computational Geometry*, 46(7):818–830, 2013.
- [6] Sergey Brin and Lawrence Page. Reprint of: The anatomy of a large-scale hypertextual web search engine. *Computer Networks*, 56(18):3825–3833, 2012.
- [7] Christian S. Collberg, Stephen G. Kobourov, Jasvir Nagra, Jacob Pitts, and Kevin Wampler. A system for graph-based visualization of the evolution of software. In *Proceedings of the ACM Symposium on Software Visualization (SOFTVIS)*, pages 77–86. ACM, 2003.
- [8] David P. Dobkin, Emden R. Gansner, Eleftherios Koutsofios, and Stephen C. North. Implementing a general-purpose edge router. In *Proceedings of the 5th International Symposium on Graph Drawing (GD)*, volume 1353 of *LNCS*, pages 262–271. Springer, 1997.
- [9] David Douglas and Thomas Peucker. Algorithms for the reduction of the number of points required to represent a digitized line or its caricature. *The Canadian Cartographer*, 10(2):112–122, 1973.
- [10] Tim Dwyer and Lev Nachmanson. Fast edge-routing for large graphs. In *Proceedings of the 17th International Symposium on Graph Drawing (GD)*, volume 5849 of *LNCS*, pages 147–158. Springer, 2009.
- [11] David Eppstein, Michael T. Goodrich, Ethan Kim, and Rasmus Tamstorf. Motorcycle graphs: Canonical quad mesh partitioning. *Comput. Graph. Forum*, 27(5):1477–1486, 2008.
- [12] Emden R. Gansner, Yifan Hu, and Stephen G. Kobourov. Gmap: Visualizing graphs and clusters as maps. In *Proceedings of the IEEE Pacific Visualization Symposium (PacificVis)*, pages 201–208. IEEE Computer Society, 2010.
- [13] Emden R. Gansner, Yifan Hu, Stephen C. North, and Carlos Eduardo Scheidegger. Multi-level agglomerative edge bundling for visualizing large graphs. In *Proceedings of the IEEE Pacific Visualization Symposium (PacificVis)*, pages 187–194. IEEE, 2011.
- [14] Emden R. Gansner and Yehuda Koren. Improved circular layouts. In *Graph Drawing*, pages 386–398. Springer, 2006.

- [15] Yoav Giyora and Haim Kaplan. Optimal dynamic vertical ray shooting in rectilinear planar subdivisions. *ACM Transactions on Algorithms*, 5(3), 2009.
- [16] Leonidas J. Guibas and Jorge Stolfi. On computing all north-east nearest neighbors in the  $l_1$  metric. *Information Processing Letters*, 17(4):219–223, 1983.
- [17] Danny Holten and Jarke J. van Wijk. Force-directed edge bundling for graph visualization. *Comput. Graph. Forum*, 28(3):983–990, 2009.
- [18] Y. Hu. Efficient and high quality force-directed graph drawing. *The Mathematica Journal*, 10:37–71, 2005.
- [19] Mirza Klimenta and Ulrik Brandes. Graph drawing by classical multidimensional scaling: New perspectives. In *Proceedings of the 20th International Symposium on Graph Drawing (GD)*, volume 7704 of *LNCS*, pages 55–66. Springer, 2012.
- [20] Antoine Lambert, Romain Bourqui, and David Auber. Winding roads: Routing edges into bundles. *Comput. Graph. Forum*, 29(3):853–862, 2010.
- [21] Lev Nachmanson, Roman Prutkin, Bongshin Lee, Nathalie Henry Riche, Alexander E. Holroyd, and Xiaoji Chen. Graphmaps: Browsing large graphs as interactive maps. In *Proceedings of the 23rd International Symposium on Graph Drawing & Network Visualization (GD)*, volume 9411 of *LNCS*, pages 3–15. Springer, 2015.
- [22] J. B. Orlin. A faster strongly polynomial minimum cost flow algorithm. *Operations Research*, 41:377–387, 1993.
- [23] James B. Orlin and Balachandran Vaidyanathan. Fast algorithms for convex cost flow problems on circles, lines, and trees. *Networks*, 62(4):288–296, 2013.
- [24] Sergey Pupyrev, Lev Nachmanson, Sergey Bereg, and Alexander E. Holroyd. Edge routing with ordered bundles. In *Proceedings of the 19th International Symposium on Graph Drawing (GD)*, volume 7034 of *LNCS*, pages 136–147. Springer, 2011.
- [25] Laurens van der Maaten and Geoffrey E. Hinton. Visualizing data using t-SNE. *Journal of Machine Learning Research*, 9:1–48, 2008.
- [26] Laurens van der Maaten and Geoffrey E. Hinton. Visualizing non-metric similarities in multiple maps. *Machine Learning*, 87(1):33–55, 2012.

## Appendix A

In this section we show a GraphMaps system based on H-tree and analyze its quality, which will reveal the challenges of constructing GraphMaps.

An H-tree of order  $k$ , denoted by  $H_k$  is defined recursively, as follows: If  $k = 0$ , then  $H_0$  is a geometric graph resembling the letter  $H$ , where each vertical edge is of length one, and the horizontal edge is of length two. For  $k > 0$ ,  $H_k$  is constructed by joining four copies of  $H_{k-1}$  at the four endpoints of  $H_1$ , as shown in Figure 7(a).

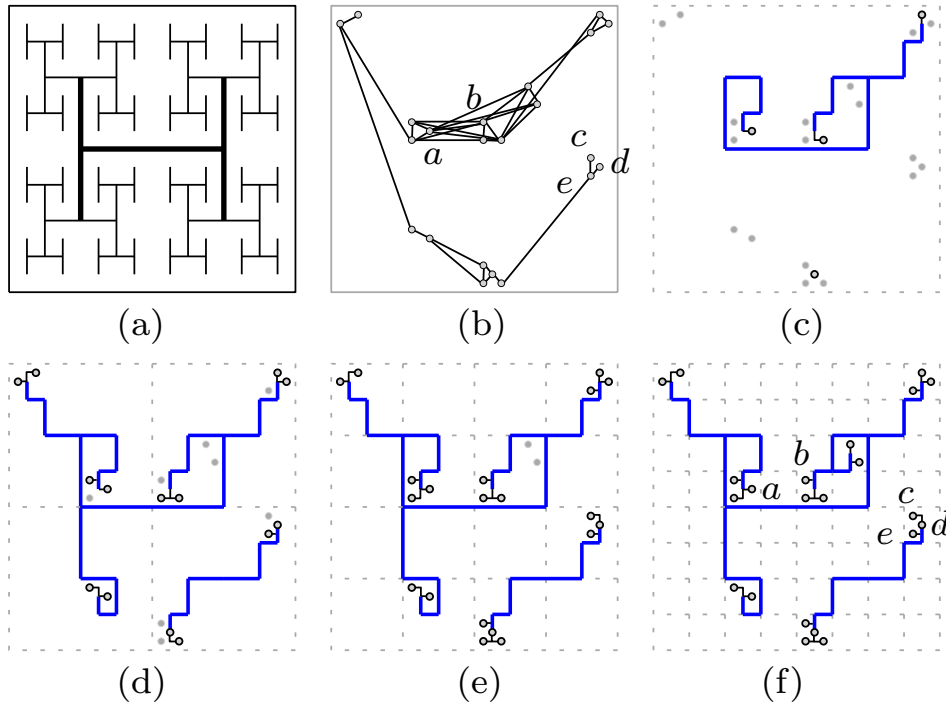


Figure 7: (a)  $H_3$ . (b)  $G$ . (c–f) A GraphMaps visualization of  $G$  based on H-tree.

Assume that we want to visualize a graph  $G$  with  $n = 21$  vertices using GraphMaps within zoom level at most four, i.e.,  $z_{max} = 4$ . The node positions are given as in Figure 7(b). For simplicity assume that all the vertices are of same priority, and the node quota  $Q_n$  per tile is four. Select  $Q_n$  nodes in the first zoom level (e.g., Figure 7(c)). For each edge  $(v, w)$  in  $G$ , we first draw the path of  $H_3$  that connects the corresponding tiles in the lowest zoom level, and then connect the vertices to the paths using a minimal length orthogonal path of at most one bend. The path that connects two tiles has at most  $O(z_{max})$  rails. Consequently, the number of rails per edge is at most  $O(z_{max})$ .

For any tile  $T$  at zoom level  $z$ ,  $T$  contains the rails that connect the nodes of  $T$  to  $H_3$ , and the rails of  $H_3$  that intersects  $T$ . The rails that connect the nodes of  $T$  to  $H_3$  is at most  $2Q_n$ , and the rails of  $H_3$  that intersects  $T$  is at most  $Q_n \cdot O(z_{max})$ , i.e., at most  $O(z_{max})$  rails to connect a node to  $H_1$ . Therefore, the number of rails per tile is bounded by  $Q_n \cdot O(z_{max})$ .

Compared to  $n$ , the parameters  $Q_n$  and  $Z_{max}$  are very small in practice. Hence the above technique ensures that the edges are drawn with small number of bends, the angular resolution at the nodes and junctions is large, and the degree of the nodes and junctions are small. However, this visualization is not very appealing due to the following reasons:

- Since the line segments are orthogonal, they create many sharp corners that unnecessarily attracts viewers attention (e.g., when the corner does not contain any node).
- Some edges may pass through vertices creating ambiguity, e.g., in Figure 7(f), the edge  $(c, e)$  passes through  $d$ , creating a false impression that  $c, d$  are adjacent in  $G$ .

- The edge stretch factor could be very large, as shown in Figure 7(f), the factor is at least 9, i.e., between  $a$  and  $b$ .
- The visualization does not make any effort to reduce abrupt view change between successive zoom levels.

## Appendix B

### Proof of Lemma 3

Define for each point  $w \in P$ , a set of eight non-overlapping cones as follows: The central angle of each cone is  $45^\circ$  and the cones are ordered counter clockwise around  $w$ . The first cone lies in the first quadrant of  $w$  between the lines  $y = x + w_x$  and  $y = 0$ , as shown in Figure 8(a). Guibas and Stolfi [16] showed that in  $O(n \log n)$  time, one can find for every point  $w \in P$  the nearest neighbor of  $w$  (according to the Manhattan Metric) in each of the eight cones of  $w$ . Assume that  $\delta_y = \{\min_{\{a,b\} \in P, \text{ where } a_y \neq b_y} |a_y - b_y|\}$ , which can be computed in  $O(n \log n)$  time by sorting the points according to  $y$ -coordinates.

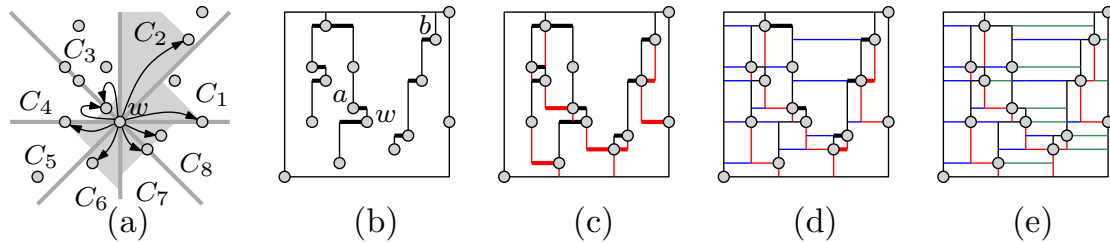


Figure 8: (a) A point set  $P$  and the nearest neighbor of  $w$  in each of the eight cones around  $w$ . (b–e) Construction of the mesh of  $P$ , while processing (b) top rays, (c) bottom rays, (d) left rays and (e) right rays.

We construct  $M$  in four phases. The first phase iterates through the top rays of the each point  $w$  and finds the point  $w'$  closest to  $l(h)_w$  (in Manhattan metric) such that  $|w'_x - w_x| \leq |w'_y - w_y|$ . Note that if such a  $w'$  exists, then one of the horizontal rays  $r'$  of  $w'$  would reach the point  $(w_x, w'_y)$  before the top ray  $r$  of  $w$  (while all rays are grown in a uniform speed). According to the definition of the competition mesh, we can continue the ray  $r'$  and stop growing the ray  $r$ . If no such  $w'$  exists, then  $r$  must hit  $R(P)$ .

To find the point  $w'$ , it suffices to compare the Manhattan distances of the nearest neighbors in the second and third cones of  $w$  (breaking ties arbitrarily). Since the nearest neighbors at each cone can be accessed in  $O(1)$  time, we can process all the top rays in linear time. Figure 8(b) shows the junctions and nodes created after the first phase, where all the rays that stopped growing are shown in thin lines. The nearest neighbors in the second and third cones of  $w$  are  $a$  and  $b$ , respectively. Since  $a$  is closer to  $l_h(w)$  than  $b$ , the top ray of  $w$  does not grow beyond  $(w_x, a_x)$ . The second phase processes the bottom rays in a similar fashion, e.g., see Figure 8(c). Both the first and second phase use a ray shooting data structure to check whether the current ray already hits an existing ray. We describe this data structure in the next paragraph while discussing phase three. Let the planar subdivision at the end of phase two be  $S$ .

In the third phase, we grow each left ray until it hits any other vertical segment in  $S$ , as follows: For each vertical edge  $ab$  in  $S$ , construct a segment  $a'b'$  by shrinking  $ab$  by  $\delta_y/3$  from both ends. For each node and junction  $w$ , construct a segment  $w_1w_2$  such that  $w_1 = (w_x, w_y - \delta_y/4)$  and  $w_2 = (w_x, w_y + \delta_y/4)$ . Let  $S_v$  be the constructed segments. Note that the segments in  $S_v$  are non-intersecting. Giyora and Kaplan [15] gave a ray shooting data structure  $D$  that can process  $O(n)$  non-intersecting vertical rays in  $O(n \log n)$  time, and given a query point  $q$ ,  $D$  can find in  $O(\log n)$  time the segment (if any) in  $S_v$  immediately to the left of  $q$ . Furthermore,  $D$  supports insertion and deletion in  $O(\log n)$  time. For each point  $q \in P$  in the increasing order of  $x$ -coordinates, we shoot a leftward ray  $r$  from  $q$ , and find the first segment  $ab$  hit by the ray.

Assume that  $a_y < b_y$  and  $r$  hits  $ab$  at point  $x$ . We update the subdivision  $S$  accordingly, then delete segment  $ab$  from  $D$ , and insert segment  $xb$  in  $D$ . Note that these updates keep all the segments in  $D$  non-intersecting. Since there are  $O(n)$  left rays, processing all these rays takes  $O(n \log n)$  time. Figure 8(d) illustrates the third phase.

The fourth phase processes the right rays in a similar fashion, e.g., see Figure 8(e). Since the preprocessing time of the data structures we use is  $O(n \log n)$ , and since each phase runs in  $O(n \log n)$  time, the construction of the computation mesh takes  $O(n \log n)$  time in total.